On the fractal dimension of self-affine profiles

1994 J. Phys. A: Math. Gen. 27 8079

(http://iopscience.iop.org/0305-4470/27/24/018)

J. Phys. A: Math. Gen. 27 (1994) 8079–8089. Printed in the UK

On the fractal dimension of self-affine profiles

J G Moreira†, J Kamphorst Leal da Silva† and S Oliffson Kamphorst‡

† Departamento de Física, Instituto de Ciências Exatas, Universidade Federal de Minas Gerais, CP 702, 30161-970 Belo Horizonte, Brazil

‡ Departamento de Matemática, Instituto de Ciências Exatas, Universidade Federal de Minas Gerais, CP 702, 30161-970 Belo Horizonte, Brazil

Received 13 June 1994, in final form 23 September 1994

Abstract. One-dimensional profiles $f(x)$ can be characterized by a Minkowski–Bouligand dimension D and by a scale-dependent generalized roughness $W(f,\epsilon)$. This roughness can be defined as the dispersion around a chosen fit to $f(x)$ in an ϵ-scale. It is shown that $D = \lim_{\epsilon\to 0}[2 - \ln W(f,\epsilon)/\ln\epsilon]$ holds for profiles nowhere differentiable. This establishes a close connection between the roughness and the fractal dimension and proves that $D = 2 - H$ for self-affine profiles (H is the roughness or Hurst exponent). Two numerical algorithms based on the roughness, one around the local average $(f(x))_\epsilon$ (usual roughness) and the other around the local RMS straight line (a generalized roughness), are discussed. The estimates of D for standard self-affine profiles are reliable and robust, especially for the last method.

1. Introduction

The seemingly complex forms of nature can be described in terms of the concepts of fractal geometry [1]. These forms often present statistical scale invariance and can be characterized by a few parameters (fractal dimensions and scaling exponents). In the case that the scale invariance comes from an isotropic length-scale transformation the object is called a self-similar fractal. We can cite as examples coastlines [1], percolation clusters [1, 2], colloidal aggregates [3] etc. When an object is invariant under a transformation with different length scales in different directions it is a self-affine fractal [4]. Recent works have demonstrated that a wide class of processes lead to objects with self-affine properties: plots of random walks [1, 2], interfaces in far-from-equilibrium systems [5, 6] and interfaces resulting from growth processes [5–8]. An interface is often characterized by the roughness $W(f,\epsilon)$, which is defined as the fluctuation of the height f over a length scale ϵ. For self-affine interfaces, the roughness $W(f,\epsilon)$ scales with the linear size ϵ of the surface by an exponent H, called the roughness or Hurst exponent.

In this paper we consider the connection between generalized roughness and the fractal dimension for one-dimensional interfaces (profiles) $f(x)$. Profiles are characterized by a fractal dimension D (Minkowski–Bouligand dimension or box dimension [1]) and by a roughness or Hurst exponent H. Essentially the fractal dimension is related to the scaling properties of the area of a cover for the profile and the Hurst exponent measures the scaling of the average of a local roughness $w(x,\epsilon)$, evaluated in an ϵ-neighbourhood of x. We show that the average generalized roughness $W(f,\epsilon) = \int_0^1 w(x,\epsilon)\,dx$ is related to the fractal dimension by $D = \lim_{\epsilon\to 0}[2 - \ln W(f,\epsilon)/\ln\epsilon]$. This result allows us to define two numerical algorithms. The first one is based on the usual roughness, namely the roughness

0305-4470/94/248079+11$19.50

around the local average height $\langle f(x)\rangle_\epsilon$. The second is based on a roughness around the local RMS straight line. These methods are tested on self-affine curves with known fractal dimensions: the Weierstrass function and the fractional Brownian motion. The estimates of D are then compared with the ones obtained from the methods of the literature.

This paper is organized as follows. In the next section we discuss briefly some known aspects of self-affinity and roughness. The Weierstrass function and the fractional Brownian motion are also presented. The mathematical aspects of the connection between the generalized roughness and the Minkowski–Bouligand dimension are discussed in section 3. In section 4 we define two numerical algorithms based on the roughness and discuss the results obtained. A summary of our results is presented in the final section.

2. Self-affinity and roughness concepts

In order to discuss the differences between self-similar and self-affine fractals, let us present briefly some relevant definitions. We consider fractals built by recurrence relations (deterministic fractals) or by means of stochastic processes (statistical fractals). A more detailed discussion can be found in [1,2].

Consider a bounded set S in a Euclidean space of dimension d. The position of each point in S is described by a vector $x = (x_1, x_2, \ldots, x_d)$. An *affine transformation* of real scaling ratios $r_1, r_2, \ldots r_d$ ($0 < r_i < 1$, with $i = 1 \ldots d$) takes each element of S with position x into an element of the set $r(S)$ with position $r(x) = (r_1 x_1, r_2 x_2, \ldots, r_d x_d)$. The set S is *self-affine* if it is the union of N distinct subsets congruent to $r(S)$. By congruent we mean identical under translations and/or rotations. S is *statistically self-affine* if its subsets are statistically congruent to $r(S)$.

When all the scaling ratios are equal ($r_1 = r_2 = \cdots = r_d = r$) we have a *similarity transformation*. In a similar way, the set S can be classified as *self-similar* or *statistically self-similar*. We can associate several dimensions to a self-similar set like the similarity dimension or the box dimension [1,2]. On the other hand, it is not so easy to associate a dimension to a self-affine set [1,9]. In fact, we can obtain different dimensions depending on the way one measures it.

Further, let us recall the definition of the box dimension. It is defined from the scaling of the average number $\langle N_{\mathrm{box}}(L)\rangle$ of d-dimensional boxes of linear size L needed to cover the set S, namely

$$\langle N_{\mathrm{box}}(L)\rangle \sim L^{-D}. \tag{1}$$

Here D is the box dimension. For deterministic self-similar fractals, such as the Koch curve, the Sierpinsky gasket or the standard Cantor set, both the similarity and the box dimension are equal and evaluated exactly, because the scaling is exact. For statistical fractals the dimensions are evaluated by using scaling arguments.

In order to illustrate the differences in the evaluation of dimensions of self-affine sets, let us introduce two standard examples of such sets. The first is the Weierstrass function (WF) $f_H(x)$, defined as

$$f_H(x) = \sum_{n=-\infty}^{\infty} b^{-nH}\left[1 - \cos\left(b^n x\right)\right] \tag{2}$$

where $b > 1$ and $0 < H < 1$. Typical graphs of this function are shown in figure 1. Note that the WF has a scaling behaviour with different scaling ratios, since $f_H(bx) = b^H f(x)$.

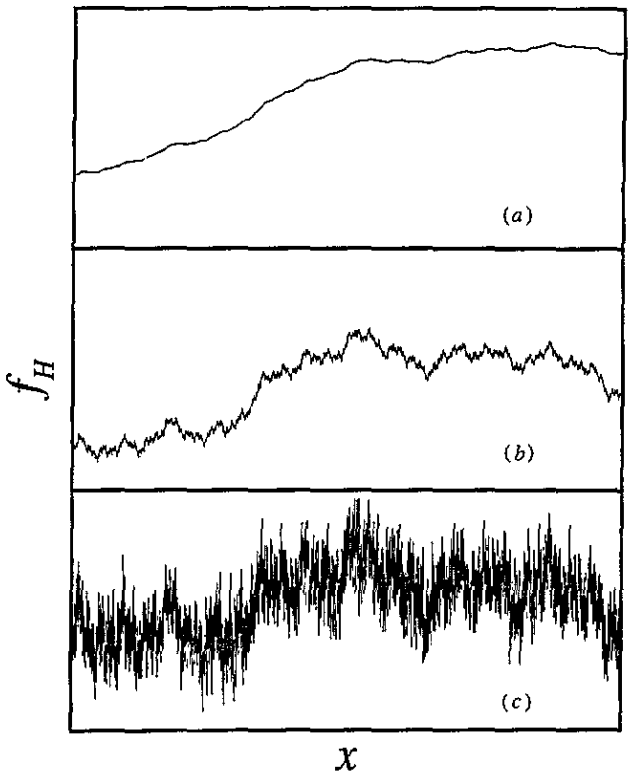

Figure 1. The Weierstrass function with $b = 2.1$ in the interval $[0.60, 0.61]$ for (*a*) $H = 0.9$, (*b*) $H = 0.5$ and (*c*) $H = 0.1$.

The second is the trace $B_H(t)$ of the fractional Brownian motion (FBM). $B_H(t)$ is a single-valued function of one variable (t) and its increments $\Delta B_H(\Delta T) = B_H(t_2) - B_H(t_1)$ have a Gaussian distribution. The variance of this distribution is given by

$$\langle \Delta B_H^2(\Delta t) \rangle \sim \Delta t^{2H} \tag{3}$$

with $0 < H < 1$, $\Delta t = |t_2 - t_1|$ and where $\langle \cdots \rangle$ denotes the ensemble average. There are several algorithms to generate the FBM. We use an algorithm described in Feder [2, p 174, equation (9.25)]. In figure 2 we show some typical traces. The FBM is a statistical self-affine object because of its scaling properties. If Δt is changed by a factor r, the increments ΔB must be changed by a different factor r^H, since

$$\langle \Delta B_H^2(r\Delta t) \rangle \sim r^{2H} \langle \Delta B_H^2(\Delta t) \rangle . \tag{4}$$

Now it is easy to obtain the box dimension of the FBM by using *scaling arguments* [2, 9]. Essentially, we evaluate the number of boxes needed to cover the trace of $B_H(t)$ in a time span T and a vertical range B. If we use small boxes we obtain the so-called *local box dimension* $D = 2 - H$. On the other hand, if we use boxes which are not small with respect to the vertical range, we obtain the *global dimension* $D = 1$. Moreover, if we measure the perimeter of the trace using a yardstick, we obtain different values for the local and global dimension (the so-called divider dimensions) [2]. If we evaluate the dimension by considering the intersection of $B_H(t)$ with the time axis (the zero-set of the FBM) we find

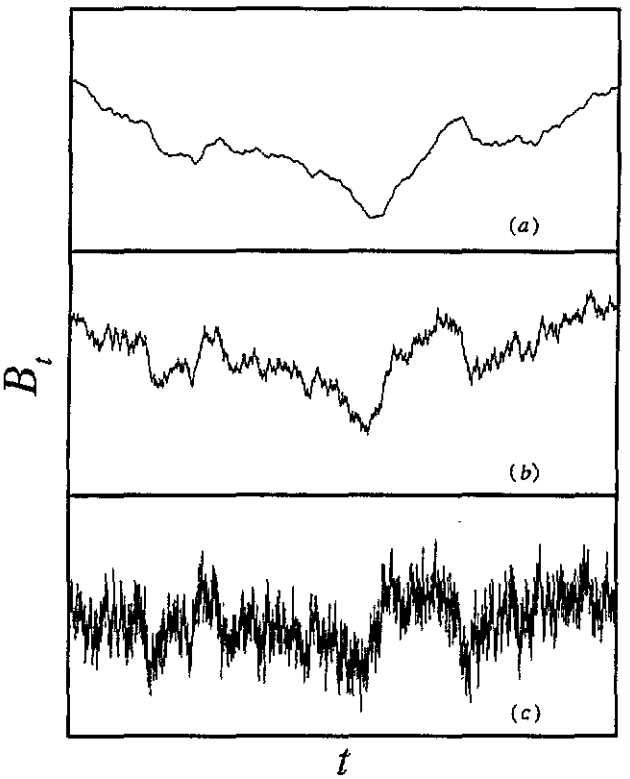

Figure 2. The fractional Brownian motion trace with $n = 8$ and $M = 700$ for (*a*) $H = 0.9$, (*b*) $H = 0.5$ and (*c*) $H = 0.1$.

$D = 2 - H$, in agreement with the local box dimension. Perhaps this last way of finding D is the least ambiguous one for associating a fractal dimension to a self-affine fractal [9]. In the next section we will consider the *direct evaluation*, instead of using scaling arguments, of the local Minkowski–Bouligand dimension (which is, in this case, completely equivalent to the local box dimension).

In many circumstances the interface $f(x)$ generated from a smooth surface by some stochastic process becomes rough. These interfaces can be characterized by a roughness $W(f, L)$, which is defined as the fluctuation around the average of the height f at scale L, namely

$$W^2(f, L) = \left\langle f^2(x) \right\rangle_L - \langle f(x) \rangle_L^2 . \tag{5}$$

where $\langle \cdot \rangle_L$ means an average over x in a scale L.

If we consider the trace of the FBM with a time span L, the roughness behaves like

$$W(B_H, L) \sim L^H \tag{6}$$

where H is the Hurst exponent. This usual roughness is evaluated around the *average height*. In the next section we show that the roughness can be generalized as the fluctuation around other interpolating functions. In particular, we can consider the local best linear fit to $f(x)$ and characterize the roughness as the fluctuations around this best linear fit.

3. The roughness exponent and the fractal dimension

In this section we present a proof of the relation $D = 2 - H$ for arbitrary profiles. Although this relation has long been known for exact self-affine profiles [10], and can also be derived from scaling arguments for statistical self-affine profiles such as the fractional Brownian motion [2, 9], there is no rigorous proof, at least to our knowledge, that it works in the general case. In particular, our result can be applied to any experiment [11, 12] without any assumptions of the statistical properties of the local scaling ratios. We should point out that for the case of statistical fractals, even the notion of fractal dimension can be viewed as a first approximation to the microscopic structure, and a multi-fractal analysis [2, 5–7] is necessary. Our proof relies on the fact that the fractal dimension, as well as the roughness exponent, measures how far a fractal curve is from any smooth function which one uses to approximate it.

Mathematically we define a profile or interface as the graph G_f of a continuous function f of a real variable x. Without loss of generality, we fix its domain of definition as the interval $[0, 1]$. We are interested in the evaluation of the fractal dimension of the graph G_f. We shall investigate the Minkowski–Bouligand dimension [13], which is equivalent to the box dimension [10]. Although these definitions of dimension characterize the local fractal properties of profiles, they can differ from the Hausdorff dimension [2, 4, 7]. In this work we do not evaluate the Hausdorff dimension.

Tricot *et al* [14] have demonstrated the equivalence between the box and Minkowski–Bouligand dimensions by using the notion of generalized covers. Covering the profile with figures of linear size ϵ, and calling $|U(\epsilon)|_2$ the area of such a cover, the fractal dimension is given by

$$D = \lim_{\epsilon \to 0} \left[2 - \frac{\ln |U(\epsilon)|_2}{\ln \epsilon} \right]. \tag{7}$$

The value of D is the same for all generalized covers using different geometric figures. Suitable figures should satisfy some non-distortion relations, for example, the figures are discs of radius ϵ centred on $(x, f(x))$ in the Minkowski–Bouligand cover and squares in the box-dimension evaluation. The numerical algorithms resulting from the Minkowski–Bouligand and box dimensions have been analysed in Dubuc *et al* [15]. The estimates obtained for D were poor when these algorithms were applied to profiles with known dimensions. It was found that the basic problem was the 'thickness' of the covers. In order to develop better numerical algorithms, Dubuc *et al* [15] have introduced two alternate ways of evaluating the fractal dimension: the *horizontal structuring element method* and the *variation method*. Both are based on the idea of building covers with intervals instead of geometrical figures. The first uses horizontal segments and the second vertical ones.

For further use, let us present briefly the variation method [14, 15]. Since we are interested in fractal graphs, we can assume that f is nowhere or almost nowhere differentiable. It is known that the graph of f has dimension 1 if its derivative is continuous. This is also the case if f is of bound variation ($\sum_{i=0}^{m-1} |f(x_i) - f(x_{i+1})|$ limited for all partitions $0 = x_0 < x_1 < \cdots < x_m = 1$) [16]. The possibility of a continuous function to have a graph of dimension strictly greater than 1 is thus related to the so-called ϵ-oscillation $v(x, \epsilon)$ of the function f, namely

$$v(x, \epsilon) = \sup_{x' \in R_\epsilon(x)} f(x') - \inf_{x' \in R_\epsilon(x)} f(x'). \tag{8}$$

and to the ϵ-variation of f in the interval [0, 1] defined by

$$V(\epsilon, f) = \int_0^1 v(x, \epsilon)\,\mathrm{d}x\,. \tag{9}$$

Here $R_\epsilon(x) = \{x' : |x - x'| < \epsilon; x' \in [0, 1]\}$ is an ϵ-neighbourhood of x.

Call $\mathcal{U}(\epsilon)$ the union of vertical segments $S(x, \epsilon) = \{x\}[\inf_{x' \in R_\epsilon(x)} f(x'), \sup_{x' \in R_\epsilon(x)} f(x')]$. This is a cover for G_f and has by definition an area equal to the ϵ-variation of f, $|\mathcal{U}(\epsilon)|_2 = |\bigcup_x S(x, \epsilon)|_2 = V(\epsilon, f)$. It can be shown then that the fractal dimension is given by

$$D = \max\left[1, \lim_{\epsilon \to 0}\left(2 - \frac{\ln V(\epsilon, f)}{\ln \epsilon}\right)\right]. \tag{10}$$

As far as fractal profiles are concerned, $D > 1$, and the fractal dimension is $2 - [\ln V / \ln \epsilon]$ in the limit $\epsilon \to 0$. This means, for instance, that the cover by vertical segments $\mathcal{U}$ can be used to calculate D. Intuitively this defines the fractal dimension as the scaling exponent of the area occupied by the graph G_f. Essentially, $V(\epsilon, f)$ measures the difference between the area under the upper approximation of f at scale ϵ and the lower approximation of f at the same scale.

The idea we now introduce is to define a finer cover by measuring a local oscillation of the function f by a local roughness, defined by

$$w^2(x, \epsilon) = \frac{1}{2\epsilon}\int_{x-\epsilon}^{x+\epsilon} [f(x') - \langle f(x')\rangle_\epsilon]^2\,\mathrm{d}x' \tag{11}$$

$$\langle f(x)\rangle_\epsilon = \frac{1}{2\epsilon}\int_{x-\epsilon}^{x+\epsilon} f(x')\,\mathrm{d}x'\,. \tag{12}$$

The average roughness is defined by $W(f, \epsilon) = \int_0^1 w(x, \epsilon)\,\mathrm{d}x$. We will show that this is related to the ϵ-variation V and then to the fractal dimension through

$$\lim_{\epsilon \to 0} \frac{\ln W(f, \epsilon)}{\ln \epsilon} = \lim_{\epsilon \to 0} \frac{\ln V(f, \epsilon)}{\ln \epsilon}\,. \tag{13}$$

Note that $\langle f(x)\rangle_\epsilon$ is a local average of the function f. Actually this local average function may be replaced by any smooth interpolating function in (11). It can be replaced by, for example, the local RMS straight line in order to have a better local fit. A sufficient condition used in the proof of (13) is that the local roughness satisfies

$$0 < w(x, \epsilon) \leqslant v(x, \epsilon) \qquad \text{for all } x \text{ and all } \epsilon > 0. \tag{14}$$

For the average of the function $\langle f(x)\rangle_\epsilon$ the condition (14) is easily verified from (8) and (11). We can see, in fact, that $w(x, \epsilon) > 0$ holds for any smooth fitting if we assume that the function f is *nowhere differentiable*. The condition $w(x, \epsilon) \leqslant v(x, \epsilon)$ means that this cover is finer than the one due to the ϵ-oscillation and therefore is a better fit to the graph G_f. Now we demonstrate that (13) holds for oscillations $w(x, \epsilon)$ satisfying (14). For every fixed $\epsilon > 0$, $w(x, \epsilon)$ is a continuous strictly positive function of x on the interval [0, 1]. Therefore we can find a δ_ϵ such that $w(x, \epsilon) \geqslant \delta_\epsilon > 0$ for all x. On the other hand, $v(x, \epsilon)$ is also continuous with regard to ϵ and x on compact sets of the plane. Then we can choose $\epsilon' < \epsilon$ such that $v(x, \epsilon') \leqslant \delta_\epsilon$ for all x. Therefore we have

$$V(f, \epsilon') \leqslant W(f, \epsilon) \leqslant V(f, \epsilon)\,. \tag{15}$$

Taking the logarithm and dividing by $|\ln \epsilon|$, and using that $|\ln \epsilon'| > |\ln \epsilon|$, we have

$$\frac{\ln V(f, \epsilon')}{\ln \epsilon'} \geqslant \frac{\ln W(f, \epsilon)}{\ln \epsilon} \geqslant \frac{\ln V(f, \epsilon)}{\ln \epsilon} \tag{16}$$

where, in fact, ϵ' depends on ϵ, but goes to zero as ϵ goes to zero. Therefore, taking the limit of (16) as $\epsilon, \epsilon' \to 0$ and using (10) we obtain that the fractal dimension D is given by

$$D = 2 - \lim_{\epsilon \to 0} \frac{\ln W(f, \epsilon)}{\ln \epsilon} . \tag{17}$$

This equation is the main result of this paper and establishes a formal connection between the roughness and the fractal dimension. For self-affine curves we have that $W(f, \epsilon) \sim \epsilon^H$, where H is the Hurst exponent, implying that $D = 2 - H$.

4. Numerical algorithms

It is straightforward to develop numerical algorithms to evaluate the dimension D for profiles by using (17). Suppose that we have $N+1$ points $f(n/N)$ $(n = 0, 1, 2 \ldots N)$ of the digitized profile. In the first method for the roughness around the mean height (MHR) we consider a ϵ-neighbourhood around each point $x = n/N$ of the digitized profile. First we evaluate the local average height $\langle f(x) \rangle_\epsilon = (1/\epsilon) \sum_{n \in \epsilon} f(n/N)$. Then we evaluate the local roughness, namely

$$w^2(x, \epsilon) = \frac{1}{\epsilon} \sum_{n \in \epsilon} \left(f\left(\frac{n}{N}\right) - \langle f(x) \rangle_\epsilon \right)^2 . \tag{18}$$

Finally, we obtain the ϵ-dependent roughness as

$$W(f, \epsilon) = \frac{1}{N+1} \sum_{x=0}^{1} w(x, \epsilon) . \tag{19}$$

This procedure is repeated for several scales ϵ and the fractal dimension D is given by the slope of the $\ln[W(f, \epsilon)/\epsilon^2] \times \ln(1/\epsilon)$ plot. Due to discreteness, the log–log plot does not give an accurate estimate of D for all scales ϵ. We have defined a smallest scale ϵ_0 and consider all scales to be of the form $\epsilon_k = c^k \epsilon_0$ $(\epsilon_k < N)$, where $c > 1$ is a constant. Then we evaluate the local slope D_i of the graph by taking a fixed number of successive points starting at k_i. When D_i is almost constant we have a reliable estimate of D. We consider the most frequent value of D_i as the best estimate for the fractal dimension. The error bar is estimated by considering the values near D_i which are significantly frequent.

Let us present the second method, the roughness around the RMS straight line (SLR). In this case, we again consider an ϵ-neighbourhood to each point x. We evaluate the best straight line $a_x(n/N) + b_x$ in this interval, with the coefficients a_x and b_x evaluated by the root-mean-square method. The local roughness is defined by

$$w^2(x, \epsilon) = \frac{1}{\epsilon} \sum_{n \in \epsilon} \left[f(n/N) - \left(a_x \frac{n}{N} + b_x \right) \right]^2 . \tag{20}$$

The ϵ-dependent roughness $W(f, \epsilon)$ has the same expression as the preceding case (equation (19)). The remaining steps are the same as in the first method.

In order to test the robustness and the efficiency of these algorithms, we evaluate the D-dimension of mathematical objects with well known fractal dimension. The first object is the Weierstrass function (WF), defined in (2). The local box dimension is given by $D = 2 - H$. The second object is the trace $B_H(t)$ of the fractional Brownian motion (FBM), already presented in section 2. The numerical values of D for the WF are shown in table 1. The exact fractal dimension is given in the first column; the estimates D_{VAR} obtained by using the variation method [15] are shown in the second column; the third and fourth columns show the evaluation of the fractal dimensions obtained by our first method (D_{MHR}) and

Table 1. Fractal dimensions D of profiles generated by the Weierstrass function with $b = 2.1$ in the interval [0.60, 0.61]; the profiles studied have been digitized with 20 000 points; D is the exact value and D_{VAR} is the estimate of the variation method; D_{MHR} and D_{SLR} are the results obtained from the roughness around the local average height and around the local RMS straight line, respectively. The error in the last digit is indicated between parentheses.

D	D_{VAR}	D_{MHR}	D_{SLR}
1.9	1.83(1)	1.898(1)	1.901(1)
1.7	1.655(5)	1.702(2)	1.709(1)
1.5	1.475(1)	1.500(6)	1.515(1)
1.3	1.281(1)	1.292(6)	1.319(1)
1.1	1.096(1)	1.101(3)	1.121(1)

Table 2. Fractal dimensions D of profiles generated by the fractional Brownian motion with $n = 8$ and $M = 700$; the studied profiles have 20 000 points; D, D_{VAR}, D_{MHR} and D_{SLR} are defined as in the preceding table.

D	D_{VAR}	D_{MHR}	D_{SLR}
1.9	1.80(2)	1.88(1)	1.87(1)
1.7	1.68(2)	1.725(5)	1.715(5)
1.5	1.52(2)	1.535(5)	1.525(5)
1.3	1.34(2)	1.36(2)	1.320(5)
1.1	1.22(4)	1.24(4)	1.105(5)

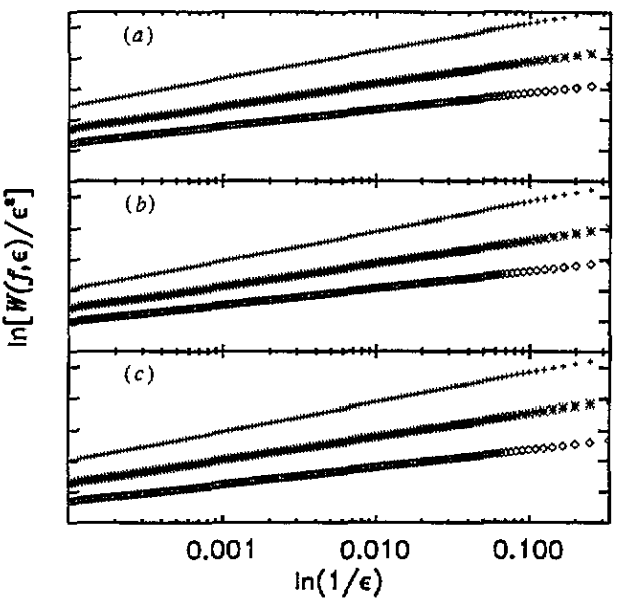

Figure 3. The $\ln[W(f,\epsilon)/\epsilon^2] \times \ln(1/\epsilon)$ plot of the Weierstrass function obtained by (*a*) the variation method, (*b*) the MHR method and (*c*) the SLR method for $H = 0.1$ (+), $H = 0.5$ (*) and $H = 0.9$ (○).

second methods (D_{SLR}). The error in the last digit is shown between parentheses. The results for the FBM are shown in table 2, which is similar to the preceding table.

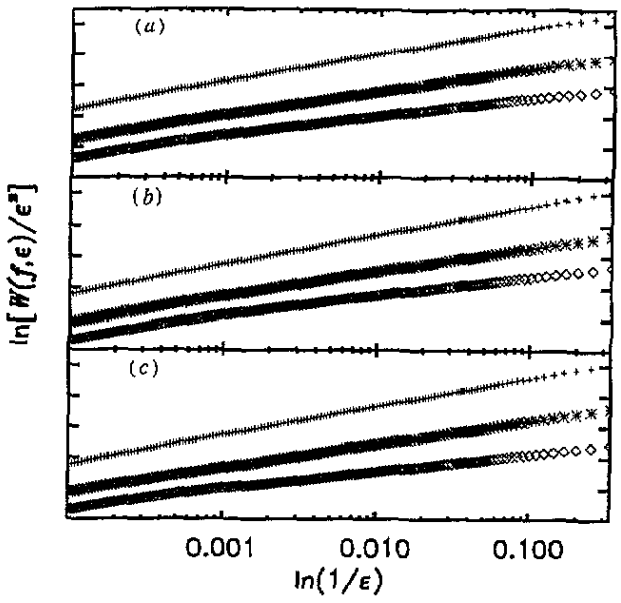

Figure 4. Figure similar to figure 3 for the fractional Brownian motion.

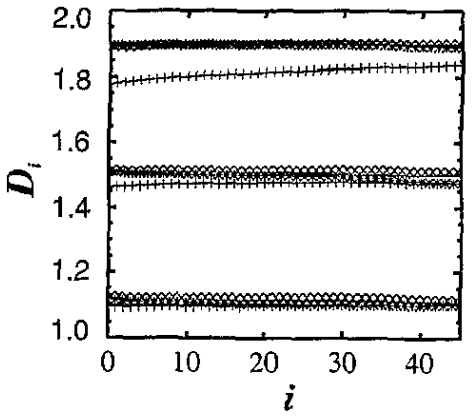

Figure 5. The graphs of the fractal dimension $D_i \times i$ of the Weierstrass function for three different values of the parameter H. The exact values are represented by full curves. Shown also are the estimates obtained by the variation (+), the MHR (*) and the SLR (◇) methods.

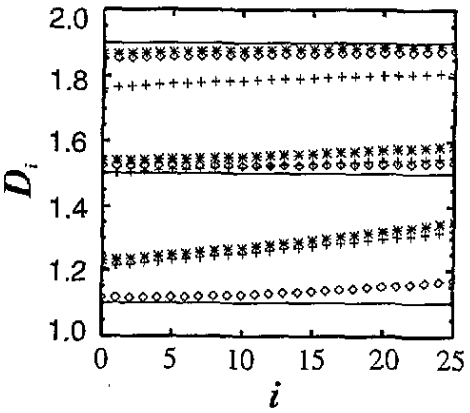

Figure 6. Figure similar to figure 5 for the fractional Brownian motion.

The $\ln[W(f,\epsilon)/\epsilon^2] \times \ln[1/\epsilon]$ plots of the WF for three values of H are depicted in figure 3. Similar plots are shown for the FBM in figure 4. From these plots we evaluate the slope D_i of several intervals of scales ϵ. The corresponding $D_i \times i$ plots are shown in figures 5 and 6.

Now let us discuss the results obtained for the WF. In figure 3 we can see that we have a very good straight line for the three methods, but some differences between them can

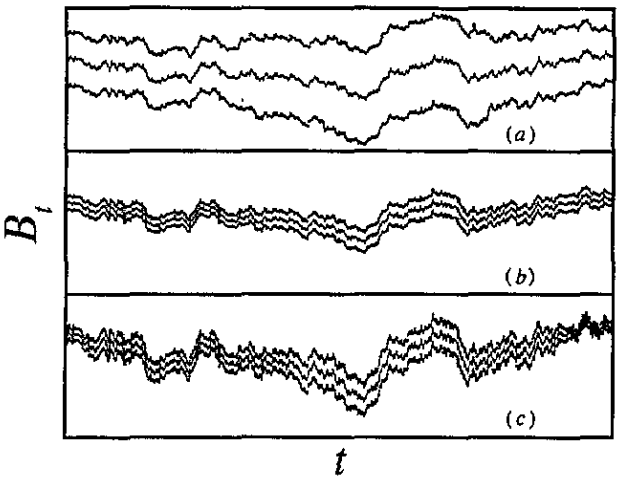

Figure 7. Covering of the FBM trace with $H = 0.5$ by the (*a*) VAR, (*b*) MHR and (*c*) SLR methods. The middle curves represent the traces, the top (bottom) curves are obtained by adding (subtracting) the local roughness $w(x, \epsilon)$ to the coordinates of the traces. For the VAR method the roughness is given by (10). The traces are digitized with 5000 points and $\epsilon = 1000$.

be seen in figure 5. The results of the variation method at low H (high roughness) only stabilize for large scales, and to a value below the expected one. For the other two methods the results are almost stable for all scales and are in good agreement with the theoretical value of D. When the roughness is small ($H \sim 0.9$), the variation method is more stable and the three methods give good results for the fractal dimension.

The results obtained by the three methods for the FBM are not as good as the ones obtained for the WF. For high roughness, the MHR and SLR methods give us a better estimate of D than the variation one. In the case where the roughness is small, none of the methods are stable for large scales, particularly the VAR and MHR methods. In these cases, the straight-line roughness method is the only one that gives a reliable estimate of the fractal dimension.

The above results can be explained as follows. Figure 7 shows the coverings of the trace of the FBM with an intermediate value of the parameter H. The scales of the plots are the same for all three methods. We can see that the covering of the SLR method is the finest and that the one for the variation method is very crude. Independent of the test function, the VAR method does not give a good estimate of D for low H because the curve is so rough (see figures 1(*c*) and 2(*c*)), implying that the cover is particularly crude. For the WF with $H \sim 0.9$ the profile is quite smooth, as shown in figure 1(*a*), and the three methods work well. On the other hand, for the FBM trace in the same range of H, the profile is also quite smooth but has some hills and valleys (see figure 2(*a*)). It means that we have a large-scale roughness, which is not taken in account by the VAR and MHR methods.

All results shown here were obtained for a particular set of parameters described in the table captions. However, we have checked the robustness of the methods by considering the WF and the FBM with other sets of parameters and found similar results. The estimates of D were obtained by visiting each point of the 20 000 ones of the digitized profile. Moreover, the results do not change when the profiles are digitized with less points. For instance, we have studied profiles with 5000 and 2000 points and observed a difference only in the

last significant digit in the case of 2000 points. Finally, we observe that in all numerical evaluations of the fractal dimensions the constant c, which defines the scales ϵ, has the value $c = 1.05$. Its value only determines the number of scales in the $\ln[W(f, \epsilon)/\epsilon^2] \times \ln(1/\epsilon)$ plots.

5. Summary

In conclusion, we have shown that the roughness is closely related to the fractal dimension (Minkowski–Bouligand or box dimensions) of profiles nowhere differentiable. In particular, we have demonstrated the relation $D = 2 - H$ for self-affine fractals. This has allowed us to present two numerical algorithms for the evaluation of the fractal dimension of one-dimensional profiles. These algorithms, based on generalized roughness, are more robust and reliable than the standard ones. This last comment applies especially to the method of the roughness around the RMS straight line. The mathematical results obtained here can be generalized for d-dimensional interfaces. In particular, the numerical algorithms for two-dimensional profiles are being developed.

Acknowledgments

The authors wish to thank P Mendes and A T Bernardes for useful discussions. This research was supported in part by Conselho Nacional de Desenvolvimento Científico e Tecnológico (CNPq) and in part by Fundação de Amparo à Pesquisa do Estado de Minas Gerais (Fapemig), Brazilian agencies.

References

[1] Mandelbrot B B 1982 *The Fractal Geometry of Nature* (San Francisco: Freeman)
[2] Feder J 1988 *Fractals* (New York: Plenum)
[3] Meakin P 1990 *J. Coll. Inter. Sci.* **134** 235
[4] Mandelbrot B B 1986 *Fractals in Physics* ed L Pietronero and E Tosatti (Amsterdam: North-Holland) p 3
[5] Stanley H E and Ostrowsky N (eds) 1988 *Random Fluctuations and Pattern Growth* (Dordrecht: Kluwer)
[6] Family F and Vicsek T (eds) 1991 *Dynamics of Fractal Surfaces* (Singapore: World Scientific)
[7] Vicsek T 1989 *Fractal Growth Phenomena* (Singapore: World Scientific)
[8] Family F 1990 *Physica* **168A** 561
[9] Voss R F 1989 *Physica* **38D** 362
[10] Mandelbrot B B 1985 *Phys. Scr.* **32** 257
[11] Rubio M A, Edwards C A, Dougherty A and Gollub J P 1989 *Phys. Rev. Lett.* **63** 1685
[12] Maloy K J, Hansen A and Hinrichsen E L 1992 *Phys. Rev. Lett.* **68** 213
[13] Bouligand G 1929 *Bull. Sci. Math.* **2** 185
[14] Tricot C, Quiniou J F, Wehbi D, Roques-Carmes C and Dubuc B 1988 *Rev. Phys. Appl.* **23** 111
[15] Dubuc B, Quiniou J F, Roques-Carmes C, Tricot C and Zucker S W 1989 *Phys. Rev.* A **39** 1500
[16] Falconer K 1990 *Fractal Geometry* (Wiley: Chichester)